Lattice dynamics and high-pressure Raman scattering studies of ferroelectric $K_2MgWO_2(PO_4)_2$

M. Maczka,[1] W. Paraguassu,[2] A. G. Souza Filho,[3] P. T. C. Freire,[3] A. Majchrowski,[4] J. Mendes Filho,[3] and J. Hanuza[5]
[1]*Institute of Low Temperature and Structure Research, Polish Academy of Sciences, P.O. Box 1410, 50-950 Wroclaw 2, Poland*
[2]*Departamento de Fisica, Universidade Federal do Maranhão, São Luis-MA, 65085-580, Brazil*
[3]*Departamento de Fisica, Universidade Federal do Ceara, P.O. Box 6030, Fortaleza-CE, 60455-970, Brazil*
[4]*Institute of Applied Physics, Military University of Technology, 2 Kaliskiego Street, 00-908 Warszawa, Poland*
[5]*Department of Bioorganic Chemistry, University of Economics, 53—345 Wroclaw, Poland*
(Received 11 April 2008; published 26 August 2008)

$K_2MgWO_2(PO_4)_2$ ferroelectric single crystal, derived from $KTiOPO_4$ (KTP) by replacement of two Ti^{4+} ions with Mg^{2+} and W^{6+} cations, was investigated at ambient pressure by micro-Raman scattering and infrared spectroscopies with a focus on polarization properties of vibrational modes. These results were analyzed based on classical lattice dynamics calculations which allowed to propose the normal-mode symmetries and assignments. In addition to the ambient pressure studies, high-pressure Raman scattering studies were performed. These studies showed the onset of a reversible first-order phase transition near 2.0 GPa which is associated with marked softening of the low wave number mode corresponding to motions of the K^+ ions. The structural changes at the phase transition are relatively weak and either the crystal exhibits transformation from the ambient pressure P1 to a high-pressure monoclinic structure or there is no symmetry change at the phase transition, i.e., this transition is isosymmetric.

DOI: 10.1103/PhysRevB.78.064116 PACS number(s): 77.80.Bh, 78.30.Hv, 77.84.Dy

I. INTRODUCTION

One of the most outstanding and widely used nonlinear-optical phosphates is $KTiOPO_4$ (KTP).[1–3] KTP undergoes a second-order displacive-type structural phase transition at 1206 K from the high-temperature paraelectric Pnan phase to a low-temperature ferroelectric $Pna2_1$ phase.[4] It was reported that the change of space group is mainly determined by the behavior of the K^+ cation but the TiO_6 octahedron also plays a role in this phase transition.[5] A soft optical mode was observed but its temperature dependence was complicated due to a coupling to a relaxation mode.[5,6] Pressure-dependent Raman and x-ray studies of KTP revealed a first-order phase transition at 5.5–5.8 GPa.[6–8] It was shown that this transition is purely displacive and it does not lead to any symmetry change, i.e., this transition is an isosymmetric phase transition.[8] It was also shown that KTP may exhibit a second phase transition near 10 GPa but nature of this transition was not established.[7]

The former studies showed that properties of KTP-type family of compounds can be greatly modified by replacement of K^+ (Ti^{4+}) or PO_4^{3-} by Rb^+, Cs^+, Tl^+ (Zr^{4+}, Sn^{4+}, Ge^{4+}) or AsO_4^{3-}, GeO_4^{4-}, SiO_4^{4-}.[1,5,9] In particular, such replacement has a significant impact on lattice instabilities and mechanism of the phase transition. For instance, replacement of K^+ by Tl^+ ions led to the appearance of a very clear soft mode typical for a displacive transition,[5] whereas the second-order phase transition in germanate analogs of KTP was shown to be both displacive and order-disorder in nature.[9]

Although the discussed above replacement of ions leads to significant changes in properties, the parent orthorhombic structure Pnan is preserved. When, however, Ti^{4+} ions are replaced with two ions of different valence state such as W^{6+} and Mg^{2+} (or Ni^{2+}, Co^{2+}, Fe^{2+}, Mn^{2+}, Cd^{2+}), the crystal structure is also modified.[10–12] For instance, the high-temperature structure of $K_2MgWO_2(PO_4)_2$ (KMWP), which is derived from KTP by replacement of two Ti^{4+} ions with Mg^{2+} and W^{6+} cations, is tetragonal, with the space group $P4_12_12$.[10–12] The polymorphism of this crystal is also much richer than that of KTP. The previous calorimetric, ionic conductivity, and dielectric studies showed that KMWP undergoes successive structural transitions at T_3=537, T_2=535, and T_1=436 K from the $P4_12_12$ tetragonal phase into the $P2_12_12_1$ orthorhombic, $P2_1$ monoclinic and P1 triclinic phases.[10–12] Below 537 K, KMWP displays ferroelastic properties, and below 535 K, in addition, ferroelectric properties.[10–12] The previous studies showed also that KMWP undergoes two additional phase transitions at T_4=637 and T_5=782 K. It was suggested that these transitions occur without any alteration of the tetragonal symmetry.[10–12] Recently, temperature-dependent studies of acoustic properties of KMWP were carried out using Brillouin technique.[13,14] These studies revealed that the phase transition at T_4 has an order-disorder nature whereas the phase transitions at T_2 and T_1 have both order-disorder and displacive nature.[13,14] They also showed that the phase transition at T_2 is induced by instability of the soft optic mode.[14]

The presented examples show that in order to understand phonon and structural properties, and obtain insight into the origin of lattice instabilities in the family of compounds related to KTP, it is necessary to perform studies of these materials as a function of composition, pressure, and temperature. In contrast to KTP and its analogs crystallizing in the orthorhombic structure, the phonon properties of the crystals derived from KTP by replacement of two Ti^{4+} ions with two ions of different valence states are unknown and the understanding of the nature of lattice instabilities is still very far from being satisfactory. We report therefore in this paper detailed ambient pressure polarized IR and Raman studies, results of lattice dynamics calculations, and pressure-dependent Raman studies of a representative member of this family of compounds, KMWP. The obtained results indicate that KMWP exhibits a first-order structural transformation at

about 2.0 GPa associated with tilts of nearly rigid PO_4^{3-} and WO_6 groups. It will be shown that this transition is driven by instability of the lowest wave number mode.

II. EXPERIMENT

Synthesis of KMWP crystals was described in our previous paper.[14]

IR studies were performed with a Biorad 575C FT-IR spectrometer. Polycrystalline spectra were measured as KBr pellets in the 1300–400 cm^{-1} region and in Nujol suspension for the 500–40 cm^{-1} region. Polarized IR spectra of a single crystal were measured in the $E\|x$ and $E\|z$ geometries (in tetragonal notation) at near normal incidence of 10° using a fixed-angle specular reflectance accessory. The Raman spectra were obtained with a triple-grating spectrometer Jobin Yvon T64000, which is equipped with a N_2-cooled charge coupled device detection system. The 514.5 nm line of an argon laser was used as excitation. An Olympus microscope lens with a focal distance of 20.5 mm and a numerical aperture of 0.35 was used to focus the laser beam on the sample surface. The high-pressure experiments were performed using a diamond-anvil cell with a 4:1 methanol:ethanol mixture as the transmission fluid. The spectrometer slits were set for a resolution of 2 cm^{-1}.

III. RESULTS AND DISCUSSION

A. Ambient-pressure polarized IR and Raman studies

KMWP structure consists of helical chains of alternately corner-linked WO_6 and MgO_6 octahedra oriented along [001], which are connected via phosphate groups to form a three-dimensional network. The K^+ cations are situated in large cavities which are connected by common edges forming an open tunnel system.[11,12] The room-temperature structure (space group P1) can be regarded as a slightly distorted modification of its tetragonal high-temperature phase (space group $P4_12_12$).[11,12] It is therefore helpful to start the analysis from the tetragonal phase. The total Brillouin zone-center optic modes of tetragonal phase include $23A_1+24A_2+25B_1+23B_2+47E$. The A_1, B_1, and B_2 modes are Raman active, A_2 modes are IR-active and E modes are both IR and Raman active. These modes can be grouped into stretching vibrations of the phosphate and WO_6 groups ($5A_1+5A_2+5B_1+5B_2+10E$), bending and librational vibrations of the phosphate and WO_6 groups ($10A_1+10A_2+10B_1+10B_2+20E$) and translations of the W^{6+}, Mg^{2+}, K^+, and PO_4^{3-} ions ($8A_1+9A_2+10B_1+8B_2+17E$). The primitive unit cell of the P1 structure contains the same number of KMWP units as the tetragonal phase. However, all atoms occupy C_1 symmetry sites and therefore all E-symmetry modes of the tetragonal phase should split in the P1 structure into doublets. Moreover, all nondegenerate modes of the tetragonal phase should become both IR and Raman active in the triclinic phase. Therefore, the modes which are only Raman or IR active in the tetragonal phase should become weakly IR or Raman active in the triclinic phase.

Figures 1 and 2 present the unpolarized (polycrystalline) and polarized (crystal) IR spectra. The polarized reflection

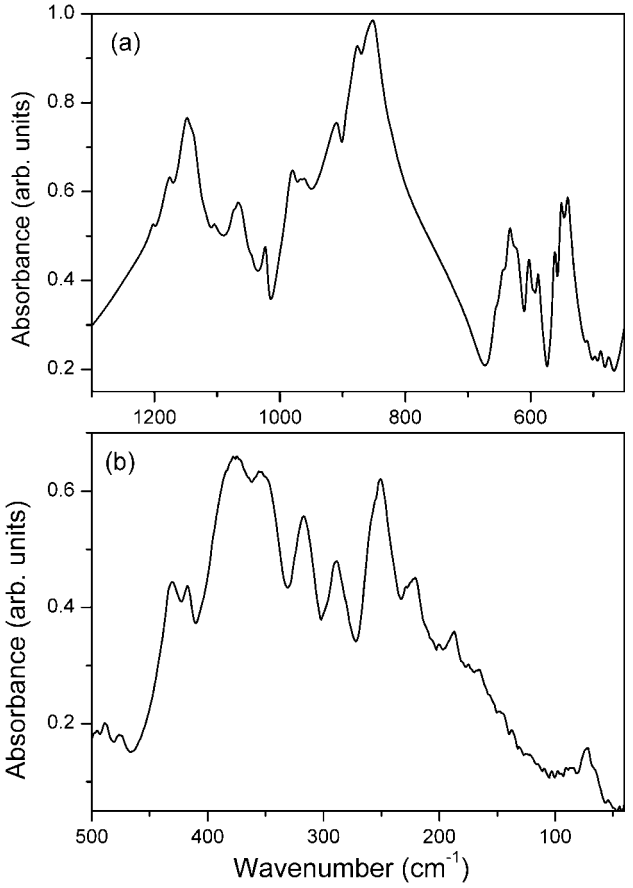

FIG. 1. Room-temperature and ambient-pressure IR spectra of polycrystalline KMWP in the (a) high and (b) low wave number region.

spectra were fitted by using four parameters model, described elsewhere,[15] in order to give information about TO and LO wave numbers. According to this model, the complex dielectric constant is expressed in terms of the IR-active modes as follows:

$$\varepsilon(\omega) = \varepsilon_\infty \prod_j \frac{\omega_{jLO}^2 - \omega^2 + i\omega\gamma_{jLO}}{\omega_{jTO}^2 - \omega^2 + i\omega\gamma_{jTO}}, \quad (1)$$

where ω_{jTO} and ω_{jLO} correspond to the resonance wave numbers of the jth TO and LO modes, respectively, and γ_{jTO} and γ_{jLO} are the corresponding damping factors. ε_∞ is the optical dielectric constant. For normal incidence, the infrared reflectivity R and the dielectric function are related by

$$R = \left| \frac{\sqrt{\varepsilon} - 1}{\sqrt{\varepsilon} + 1} \right|^2. \quad (2)$$

The plots of the calculated wave number dependence of absorption coefficient and imaginary part of the inverse dielectric function are presented in Figs. 2(b) and 2(c). The maxima of these plots correspond to TO and LO wave numbers, respectively. The results of fitting of the experimental data to the four parameter model are summarized in Table I,

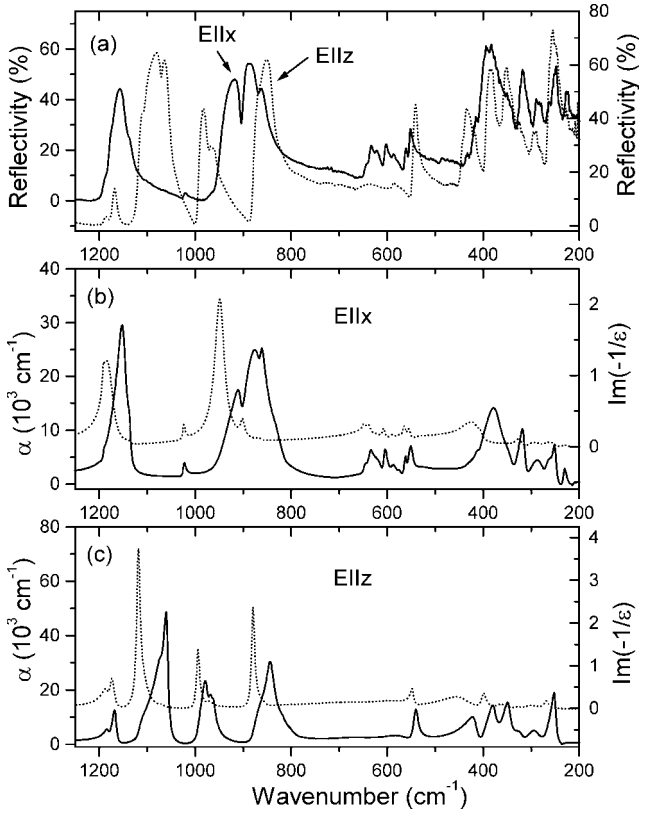

FIG. 2. (a) Reflection spectra of KMWP single crystal for $E\|x$ (solid line) and $E\|z$ (dotted line). (b) Calculated wave number dependence of the absorption coefficient α (solid line) and imaginary part of the inverse dielectric function (dotted line) for $E\|x$. (c) Calculated wave number dependence of the absorption coefficient α (solid line) and imaginary part of the inverse dielectric function (dotted line) for $E\|z$.

where oscillator strengths $\Delta\varepsilon_{\mathrm{TO}}$ are also given. Figure 3 shows the polarized Raman spectra and the observed wave numbers are listed in Table II.

Figure 2 shows that the IR spectra are very well polarized. For instance, the band at 843 cm^{-1} is observed only for the $E\|z$ polarization and the bands at 869+862 cm^{-1} for the $E\|x$ polarization. This result indicates that these bands correspond to the A_2- and E-symmetry modes of the tetragonal phase, respectively. The Raman spectra are also strongly polarized but not so pronounced as the IR spectra. The only exception is the $z(xy)\bar{z}$ spectrum which is significantly depolarized. Nevertheless, the comparison of the IR and Raman spectra allows one to identify symmetries of the majority of normal modes. It is worth to note that the strongest Raman band at 911 cm^{-1}, which can be unambiguously assigned to the Raman active A_1-symmetry mode, appears also as a weak band in the $E\|x$ IR spectrum. The activation of this mode in the IR spectrum and partial depolarization of the Raman bands can be attributed to the triclinic distortion of the parent tetragonal structure. Since the number of the observed modes for every polarization is close to that expected for the tetragonal structure, this triclinic distortion is weak.

B. Lattice dynamics calculations and assignment of modes

Since the room-temperature structure is only a slight modification of the tetragonal phase and symmetries of the majority of modes (in tetragonal notation) could be easily established, we have performed LD calculations for the tetragonal phase in order to assign the observed modes to the respective motions of atoms. The GULP code, developed by Julian J. Gale,[16,17] has been used to determine a set of classical ionic pair potential that better optimize the tetragonal structure of KMWP. The obtained set of potential has been then used to derive the initial force constants that were refined using Wilson's FG matrix method and the software package VIBRATZ developed by Dowty.[18]

The ionic model applied in the GULP code considers the material as a collection of point charges interacting by electrostatic and short-range classic potentials. The following interatomic potential is taken into account:

$$U_{ij}(r_{ij}) = \frac{z_i z_j e^2}{r_{ij}} + b_{ij} \exp\left[\frac{-r_{ij}}{\rho_{ij}}\right] - \frac{c_{ij}}{r_{ij}^6}. \quad (3)$$

The first term of this potential is related to the Coulomb forces for modeling the long-range interactions. The second term is related to the Born-Mayer type repulsive interaction for accounting the short-range forces. A van der Waals attractive interaction (third term) models the dipole-dipole interaction. z_i and z_j are the effective charges of the i and j ions, respectively, separated by the distance r_{ij}. The parameters ρ_{ij} and b_{ij} correspond to the ionic radii and ionic stiffness, respectively.

The initial lattice parameters and atomic positions for the tetragonal structure of KMWP were taken from Ref. 12. The atomic positions, potentials, and the effective charges were optimized with respect to free energy. For this model, it is usual that only cation-oxygen interactions contribute significantly to the free energy, so the remaining interactions can be neglected. The final potential coefficients and ionic charges obtained during this procedure are listed in Table III. By using this set of parameters, a good agreement between the calculated ($a=b=9.3041$, $c=10.6375$ Å) and experimental ($a=b=9.2347$, $c=10.7428$ Å) lattice parameters was obtained (the deviations were smaller than 1%).

The initial force constants were obtained by using the relation:

$$f_{ij} = -\frac{1}{r}\frac{\partial U_{ij}(r)}{\partial r}, \quad (4)$$

where $U_{ij}(r)$ represent the classical pair potential for KMWP, the indices i and j refer to interacting ions and r is the distance between them. The force obtained in the GULP program was rescaled by a factor of 1.6 in order to correct the fact that, differently from GULP, VIBRATZ program accounts only for the interactions between the first neighborhood atoms. The final Mg-O and K-O force constants were 0.144 and 0.336 mDyn/Å, respectively, and the O-O force constants were kept in the 0.98–0.56 mDyn/Å range varying with the first neighborhood distances. The W-O and P-O force-constant values were refined in order to better fit the experimental data. This refinement is necessary in order to correct

TABLE I. Dispersion parameters for the best fit to the reflectivity data of KMWP for $E\|z$ and $E\|x$ polarization.

$E\|z$					$E\|x$				
ω_{TO} (cm^{-1})	γ_{TO} (cm^{-1})	ω_{LO} (cm^{-1})	γ_{LO} (cm^{-1})	$\Delta\varepsilon_{TO}$	ω_{TO} (cm^{-1})	γ_{TO} (cm^{-1})	ω_{LO} (cm^{-1})	γ_{LO} (cm^{-1})	$\Delta\varepsilon_{TO}$
1181.8	9.8	1182.7	15.3	0.001	1191.7	6.2	1191.9	5.1	0.001
1166.0	8.2	1173.4	12.5	0.016	1148.7	15.8	1180.3	27.8	0.100
1111.3	23.5	1118.7	8.6	0.003	1136.0	7.4	1136.7	9.3	0.009
1071.6	13.0	1107.3	27.7	0.032	1023.1	6.8	1024.0	5.9	0.003
1058.4	7.6	1069.1	12.2	0.171	905.5	14.4	948.7	23.9	0.030
976.3	11.7	994.6	7.5	0.067	868.7	43.4	901.2	10.7	0.355
965.2	7.2	970.9	9.9	0.105	862.4	10.4	863.8	9.0	0.101
964.7	13.9	964.7	5.7	0.001	647.1	8.2	647.9	7.6	0.005
842.7	15.7	851.6	25.6	0.289	635.2	10.6	637.2	10.1	0.015
539.6	9.6	547.5	8.5	0.138	607.9	19.0	608.1	6.8	0.001
415.8	15.8	444.5	66.1	0.229	605.0	13.9	606.5	59.2	0.009
377.5	13.7	399.5	11.2	0.429	584.7	16.1	588.8	19.9	0.025
346.5	12.7	362.5	20.6	0.719	572.7	10.3	573.7	13.4	0.006
320.2	17.6	322.9	31.3	0.102	561.1	5.2	562.6	8.7	0.005
288.5	28.8	306.2	32.2	0.844	549.7	10.5	555.9	14.4	0.001
249.9	7.3	268.3	10.2	2.214	424.9	34.5	431.4	30.9	0.001
					410.0	10.6	416.0	20.6	0.012
					372.9	31.9	408.0	10.4	0.428
					340.5	24.5	349.5	75.9	0.131
					314.8	9.8	330.5	17.1	0.258
					270.9	27.3	305.2	31.1	1.636
					268.3	35.0	269.1	12.7	0.738
					249.8	7.2	253.1	10.1	0.625
					249.6	8.9	230.6	6.2	0.332

the lack of covalence in the ionic model. The final values used in the calculations are listed in Table IV.

The IR and Raman spectra consist of two separated regions: 820–1200 and 50–650 cm^{-1}. The bands observed in the first region can be assigned to the stretching modes and those below 650 cm^{-1} to the bending and lattice modes. Such a clear separation of two regions was not observed for KTP crystals.[7,19,20] This difference can be related to the shift of the WO_6 stretching modes toward higher wave numbers when compared to the TiO_6 stretching modes due to weak interactions of the WO_6 octahedra with Mg^{2+} ions and higher valence of the tungsten atoms with respect to titanium atoms. The former studies of a number of titanyl and niobyl phosphates showed that the symmetric and asymmetric stretching vibrations of the PO_4^{3-} ions [$v_1(PO_4)$ and $v_3(PO_4)$, respectively] are observed around 933–1000 and 970–1150 cm^{-1}, respectively.[19–23] Our LD calculations show that for KMWP the 941–976 and 1022–1202 cm^{-1} bands can be assigned to the $v_1(PO_4)$ and $v_3(PO_4)$ modes, respectively. It is worth to note that the $v_3(PO_4)$ modes are observed at higher wave numbers for KMWP than for the titanyl phosphates, for which these modes were observed in the 990–1130 cm^{-1} region.[19–21] Since the study of Na superIonic conductor (NASICON)-type phosphates revealed wave number increase with increasing covalent character of the metal-oxygen (M–O) bonds within M-O-P bridge,[24] the observed wave number increase in KMWP can be explained as a result of stronger covalent character of the W–O bonds when compared with the Ti–O bonds.

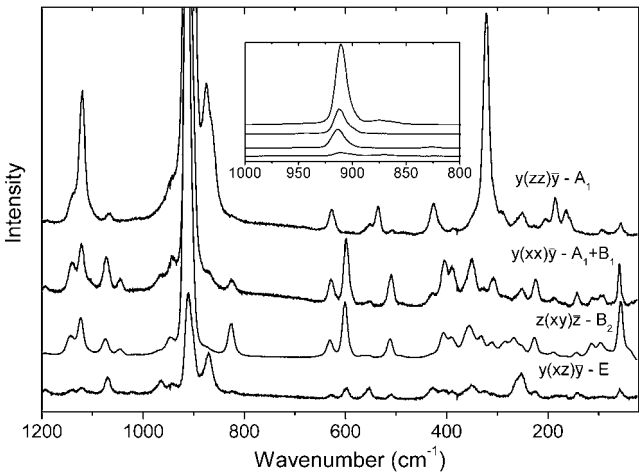

FIG. 3. Polarized Raman spectra of KMWP. The strongest bands are shown in the inset.

TABLE II. Experimental and calculated wave numbers for $K_2MgWO_2(PO_4)_2$ together with the proposed assignment.

A_1		A_1+B_1		B_2		E			A_2		IR	
RS	Cal.	RS	cal. (B_1)	RS.	cal	RS	IR	cal.	IR	cal.	pol.	Assignment
1190	1195					1193	1192	1187	1182		1202	$\nu_3(PO_4)$
1141		1141	1165	1143	1169	1142	1149	1149	1166	1145	1148+1176	
1121	1105	1122		1124	1123	1121	1136	1122	1111	1115	1141+1104	
1067		1073	1099	1075		1070		1102	1072		1072	
				1045	1023			1025	1058	1028	1066	
	1013	1045	1020			1022	1023	1016			1023	
		966	977			965		977	976	961	980	$\nu_1(PO_4)$
943	974	943		946	956	941		957	965		966	
911	928	911		913		912						$\nu_s(WO_6)$
		903		903	926	903	905				910	
875						876	869	868			876	$\nu_{as}(WO_6)$
862						869	862	867			860	
		824	811	826					843	812	852	
627	637	629	656	631	638	629	647	645		647	643	$\nu_4(PO_4)$
							635	641			633+623	
							608	611		608	603	
	585	599	601	601	578	599	605	599				
536	544		574		544		585	576	571	581	588	
					531		561	560			561	
	520		567			555	550	536	540	556	551+540	
		510	452	512	489	510		514			510+498	$\nu_2(PO_4)$+bending modes of WO_6
484	477							468	416	428	488+417	
								457			476	
426	422	430				428	425	440		392	430	
		405	404	406	455	406	410	412				
	376	388	378	391	370	387		383	378	377		$T'(PO_4)$+L(PO_4) and bending modes of the WO_6
						364	373	364			373	
	331	350	343	355	344	349	341	349	346	354	353	
				333				343				
322	322					323		321	320	317		
		308	301	311	316	307	315	306			317	
287	300			285	299			289	289	289	288	
							271	776				
		263	263	268		262	268	264		271	264	
250	240	251	243	254	234	251	250	244	250	259	251	$T'(Mg^{2+})$
								233				
		224	223	227	219	225	229	222		195	223	
205	229		212					211				
186	177		169	189	190			188		189	187	$T'(K^+)$
163	147							178				
		142	139	143	138			147		143		
						138		145				
						133		129				$T''(W^{6+})$
		112	113	114	105			117				
92	112			96				85		97	88	
	54		69		60			57		70	72	
57	27	58	37	56	22	58		29		32		$T'(K^+)$
			19					28				

TABLE III. Potential coefficients and ionic charges obtained in the lattice dynamics calculation.

	b(eV)	ρ(Å)	c(eV Å^6)
K-O	11189.8	0.238	0
Mg-O	491593.3	0.144	0
W-O	872.9442	0.444	0
P-O	877.9951	0.359	0
O-O	22764	0.149	28
Charges			
Z_K=1.0 ; Z_{Mg}=2.0; Z_W=6.0;			
Z_P=5.0 ; Z_O=−2.0			

Very interesting results have been obtained for the modes in the 800–920 cm^{-1} region. LD calculations predict that there should be three pairs of similar energy modes for KMWP at $928(A_1)+926(B_2)$, $868(E)+867(E)$, and $811(B_1)+812(A_2)$ cm^{-1}. Our Raman and IR spectra are in very good agreement with the LD calculations. First, the Raman spectrum consists in this range of 824 cm^{-1} band, which is well observed in the $y(xx)\bar{y}$ polarization but is absent in the $y(zz)\bar{y}$ and $y(xz)\bar{y}$ polarization configurations and can be, therefore, unambiguously assigned to the B_1-symmetry mode [this mode appears also in the $z(xy)\bar{z}$ spectrum since in this case the spectrum is strongly depolarized and contains also xx and yy components]. The corresponding A_2-symmetry IR mode is observed at 843 cm^{-1}. Second, there is a very clear doublet for the E-symmetry IR spectrum at 869+862 cm^{-1}. The doublet is also observed in the Raman spectra (see Table II). Third, the strongest Raman band at 911 cm^{-1} has A_1 symmetry. There is, however, a much weaker band at 903 cm^{-1} which can be most likely assigned to the B_2-symmetry mode. LD calculations show that the strongest Raman band at 911 cm^{-1} and the B_2-symmetry mode correspond to the symmetric stretching vibrations of the WO_6 octahedra whereas the remaining modes in this range correspond to the asymmetric stretching vibrations of the WO_6 octahedra.

In the bending modes region one should observe symmetric and asymmetric bending modes of the PO_4^{3-} ions [$\upsilon_2(PO_4)$ and $\upsilon_4(PO_4)$, respectively]. These modes are seen at 420 and 567 cm^{-1} for a free phosphate ion.[25] The remaining bending modes can be attributed to the WO_6 group. The former studies of a number of phosphates showed that the $\upsilon_4(PO_4)$ modes are usually well separated from the $\upsilon_2(PO_4)$ modes, giving rise to bands in the 490–670 cm^{-1} region.[22–24,26] LD calculations show that for KMWP the group of bands in the 540–643 cm^{-1} region can be unambiguously assigned to the $\upsilon_4(PO_4)$ modes. The $\upsilon_2(PO_4)$ modes were observed for the titanyl and niobyl phosphates at 370–430 cm^{-1}.[19–23] Since the $\upsilon_4(PO_4)$ modes of KMWP are observed at significantly higher wave numbers than the corresponding modes of the titanyl and niobyl phosphates, the same behavior may be expected for the $\upsilon_2(PO_4)$ modes of KMWP. Moreover, the former studies of niobyl phosphates showed that the bending modes of the NbO_6 group are observed near 450, 350, and 270 cm^{-1}.[22,23] Therefore, it is plausible to assume that also for KMWP one of the bending modes of the WO_6 group should be observed near 450–500 cm^{-1}, i.e., in the same wave number range as the $\upsilon_2(PO_4)$ mode. Our LD calculations are in agreement with this assumption since they show that the modes in the 405–510 cm^{-1} range should be assigned to the coupled modes involving bending motions of both PO_4^{3-} and WO_6 groups. They also show that the modes in the 262–388 cm^{-1} range involve translational and librational motions of the phosphate groups coupled with the bending modes of the WO_6 octahedra.

The modes below 260 cm^{-1} can be assigned to the translational motions of Mg^{2+}, K^+, and W^{6+}. Wave numbers of translational modes depend on the mass of the cation and the interaction strength with the surrounding anions. The studies of KTP located $T'(K^+)$ modes at 96 and 120 cm^{-1},[27] whereas the study of potassium-antimony phosphates located these modes below 150 cm^{-1}.[28] Translational modes of heavy W^{6+} ions were located below 150 cm^{-1} in tungstates and perovskites.[29–31] According to our LD calculations, translations of light Mg^{2+} ions contribute to the 205–251 cm^{-1} modes. Translational motions of the K^+ ions in the direction perpendicular to the tunnels (perpendicular to the c axis of the tetragonal phase) are observed in the 138–186 cm^{-1} range and the modes in the 72–133 cm^{-1} range involve large contribution of the W^{6+} translational motions. The Raman spectra show also that the lowest wave number modes are observed in the 53–58 cm^{-1} range. Very similar situation was observed for KTP, for which the lowest wave number totally symmetric mode was observed near 56 cm^{-1}.[6,7,20] This mode was shown to soften under pressure, and it was suggested that it is connected to vibrations of the K^+ ions.[6,7] Since the 57 cm^{-1} mode of KMWP also exhibits a clear softening under pressure (see discussion in Sec. IV), it is plausible to assume that this mode should also be assigned to the translational motions of the K^+ ions. Our LD calculations supports this assignment since they show that the lowest wave number Raman bands should correspond to translations of the K^+ ions along the c axis.

TABLE IV. Refined force constants for P–O and W–O bonds.

Bond	Force constant (mDyn/Å)
P–O1 and P–O2	5.3
P–O3 and P–O4	4.4
W–O5	3.7
W–O2	3.4
W–O1	3.1

C. High pressure Raman scattering studies

Once a clear picture of the vibrational properties of KMWP is obtained, we next discuss the effects of hydrostatic pressure on the structural and vibrational properties of this compound. The pressure-dependent Raman spectra are presented in Fig. 4. The comparison of these spectra with the polarized spectra presented in Fig. 3 shows that the scatter-

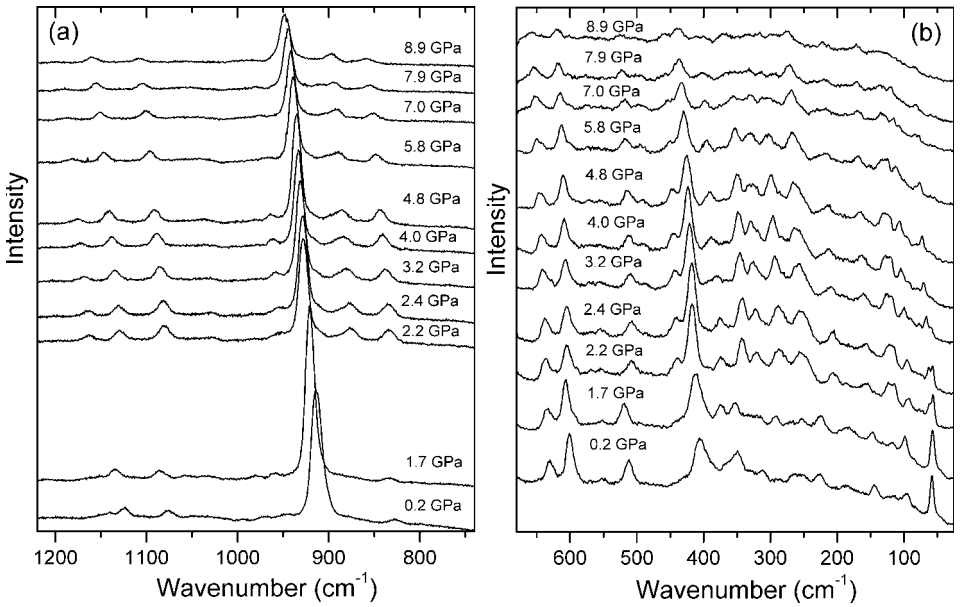

FIG. 4. Raman spectra of KMWP recorded at different pressures during compression experiments in the (a) high and (b) low wave number region.

ing geometry in the pressure-dependent studies is close to $y(xx)\bar{y}$. As the pressure increases, wave numbers of the majority of modes increase. The lowest wave number band exhibits, however, a weak softening. When pressure reaches about 2.0 GPa, a number of bands experience discontinuous wave number shifts both toward smaller and higher values. Moreover, the number of bands increases and the pressure dependence of the lowest wave number mode changes from negative to positive. The observed modifications of the Raman spectra indicate that a first-order phase transformation takes place in KMWP near 2.0 GPa. As the pressure further increases, intensities of the bands decrease continuously and their bandwidths increase. There are, however, no indications that KMWP experiences another phase transition up to 8.9 GPa. It is worthwhile to note that for the 2.2 and 2.4 GPa pressures, the lowest wave number mode, characteristic for the high-pressure phase, coexists with the lowest wave number mode characteristic for the ambient-pressure phase. This behavior could indicate that the both phases coexist in this pressure range. However, there is no evidence of the coexistence of the both phases when we observe the high wave number modes.

In order to get more insight into the mechanism of phase transitions in KMWP, we have also performed Raman studies of KMWP crystal during the decompression. Upon releasing pressure, the spectrum of the starting orthorhombic phase was recovered, as can be observed in Fig. 5, thus indicating the reversibility of the process. However, intensities of some bands of the starting phase are different before increasing the pressure and after releasing the pressure. This difference is due to some slight reorientation of the sample during the pressure release and creation of defects in the studied sample.

The overall changes in the Raman spectra can be followed by analyzing the wave number (ω) vs pressure (P) plot shown in Fig. 6. This figure shows that the pressure depen-

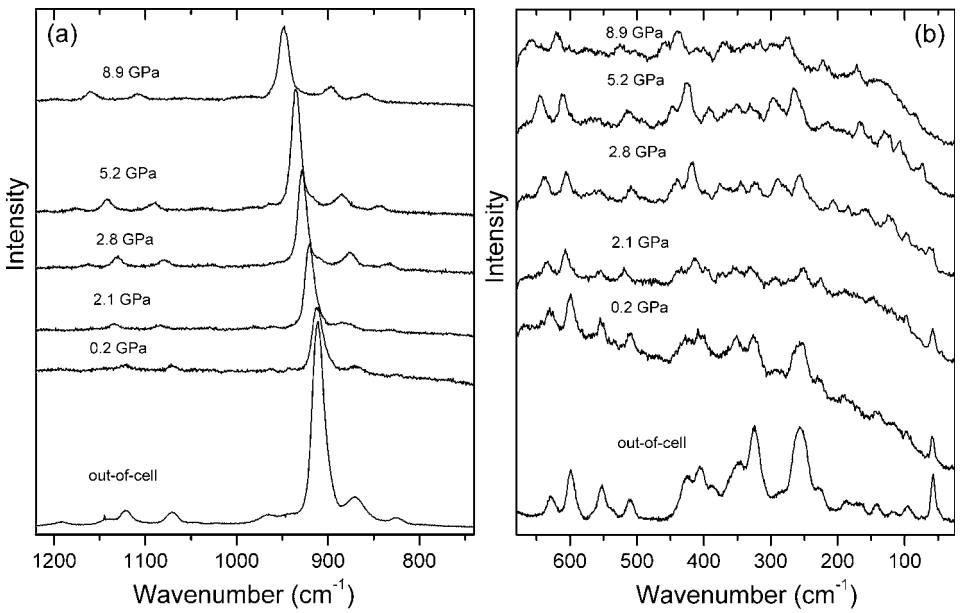

FIG. 5. Raman spectra of KMWP recorded at different pressures during decompression experiments in the (a) high and (b) low wave number region.

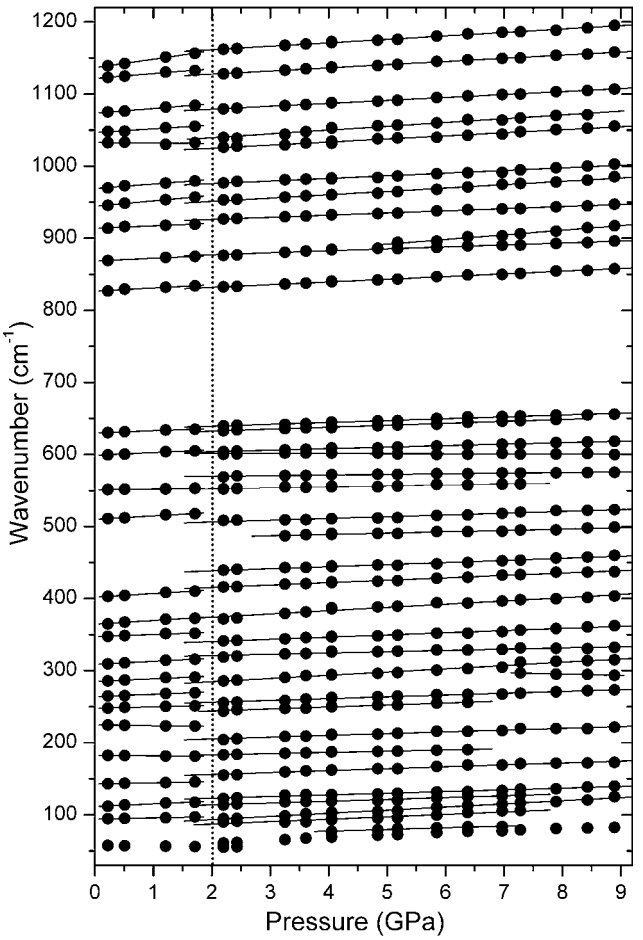

FIG. 6. Wave number vs pressure plots of the Raman modes observed in KMWP crystal for compression experiment. The vertical line indicates the pressure at which KMWP undergoes the phase transition. The solid lines are linear fits on the data to $\omega(P)=\omega_0+\alpha P$.

dence of all vibrational modes, except the lowest wave number one, can be well described using a linear function $\omega(P)=\omega_0+\alpha P$. The values of ω_0 and α are collected in Table V. The pressure dependence of the lowest wave number mode at 57 cm^{-1} is nonlinear. Figure 7 shows that squared wave number of this mode vs pressure is approximately a linear function in both pressure ranges. Linear fit on the data below (above) 2.0 GPa to $\omega^2(P)=\omega_0^2+\alpha P$ yields $\omega_0^2=33321.4(2773.2)$ cm^{-2} and $\alpha=-116.3(479.4)$ cm^{-2} GPa^{-1}.

Raman spectra show that the largest pressure coefficients are observed for the stretching vibrations of the PO_4^{3-} groups (see Table V). This result indicates that upon application of pressure more significant changes occur for the PO_4^{3-} tetrahedral groups than for the WO_6 and MgO_6 groups. When pressure reaches about 2.0 GPa, a first-order phase transition takes place, as evidenced by sudden shifts of the phonon wave numbers. Since the largest shifts are observed for the phonons assigned to the PO_4^{3-} groups, the most significant changes occur for these groups. It is worthwhile to note, however, that there is a close correspondence between the Raman spectra of the ambient-pressure and high-pressure phases. First, the observed wave number shifts are relatively small and the number of the observed modes in the stretching mode region does not change at the phase transition. At pressures higher than 4.5 GPa, a splitting of the 870 cm^{-1} band is noticed but this splitting can be attributed to a different pressure dependence of two modes, which have very close energies below 4.5 GPa, and are therefore not resolved in our pressure-dependent studies at low pressures. These two modes are, however, clearly observed in our polarized studies (see Table II). Second, in the region below 650 cm^{-1}, additional modes seem to appear above 2.0 GPa. However,

TABLE V. Pressure intercepts ω_0 and pressure coefficients α for ambient and high-pressure phases of KMWP.

$\omega(P)=\omega_0+\alpha P$			
Ambient pressure phase		High-pressure phase	
ω_0(cm^{-1})	α(cm^{-1} GPa^{-1})	ω_0(cm^{-1})	α(cm^{-1} GPa^{-1})
1136.6	11.7	1151.9	4.8
1121.7	6.6	1118.8	4.4
1073.6	6.4	1070.7	4.1
1046.5	5.3	1029.0	5.3
1032.7	−0.6	1016.3	4.3
968.9	6.3	968.4	3.6
944.3	7.5	941.7	4.6
913.7	3.5	920.1	3.0
868.4	3.8	871.7	2.7
		859.7	6.4
826.4	4.5	824.3	3.8
629.8	3.0	634.2	2.6
		627.1	2.7
598.8	3.8	599.8	2.1
		602.0	−0.2
551.2	1.0	568.0	0.9
		550.1	1.3
509.9	4.7	501.2	2.5
		481.4	1.9
		432.7	2.9
402.0	4.9	408.7	3.3
364.3	5.1	365.1	4.5
347.2	2.9	334.4	3.0
308.7	4.3	317.4	1.8
		310.8	−1.9
285.1	3.6	275.5	4.5
264.0	3.2	251.2	2.5
247.8	2.0	238.5	2.8
224.7	−1.0	200.4	2.5
182.5	−0.7	179.8	1.7
142.9	1.6	150.7	2.7
		118.3	2.3
111.6	3.6	108.7	2.6
94.2	1.6	84.7	4.4
		80.4	3.4
		68.0	2.3

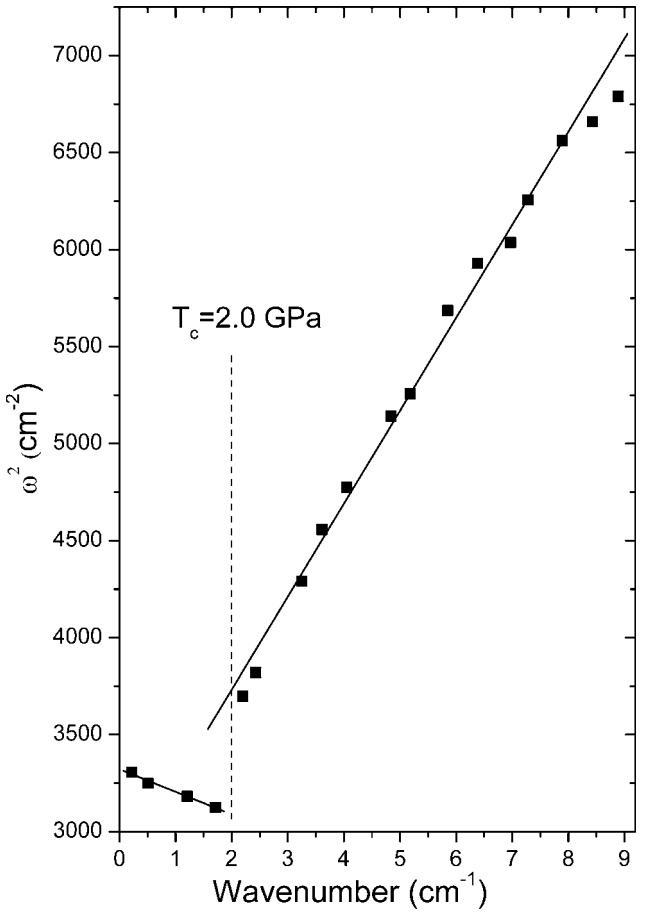

FIG. 7. The pressure dependence of the squared wave number of the soft mode for KMWP. The solid lines are linear fits on the data to $\omega^2(P)=\omega_0^2+\alpha P$.

the appearance of these modes can be explained as resulting from intensity changes of the bands, which are already present below 2.0 GPa but are very weak in the applied scattering geometry, which is close to $y(xx)\bar{y}$. For instance, our pressure-dependent spectra show below 2.0 GPa only two modes in the 450–580 cm^{-1} range at 510 and 551 cm^{-1}. Above 2.0 GPa, the 510 cm^{-1} mode shifts toward lower wave numbers and an additional mode appears near 487 cm^{-1}. The 551 cm^{-1} mode shifts to 569 cm^{-1} and an additional mode appears at 552 cm^{-1}. These additional modes can be attributed to the 484 and 536 cm^{-1} modes, which are observed in our ambient-pressure polarized studies in the $y(zz)\bar{y}$ polarization. The appearance of the additional modes indicates that the spectra of the high-pressure phase are significantly depolarized but the number of the observed modes does not change as a result of the phase transition. The close correspondence between the Raman spectra of the ambient-pressure and high-pressure phases indicates that the pressure-induced phase transition in KMWP is associated mainly with tilts of the nearly rigid PO_4^{3-}, WO_6, and MgO_6 groups. The observed depolarization of the spectra above 2.0 GPa can be most likely attributed to twinning of the crystal. Our results show also that the PO_4^{3-} and WO_6 groups are slightly more distorted in the high-pressure phase since the stretching modes of the PO_4^{3-} and WO_6 groups are observed in a slightly larger wave number ranges for the high-pressure phase than for the ambient-pressure phase (see Fig. 6).

It is worth to note that KMWP undergoes a phase transition at significantly lower pressure (about 2.0 GPa) than KTP (about 5.4 GPa).[7,8] This difference can be most likely related to less compact arrangements of the structural units in the KMWP structure. In particular, the x-ray studies showed that the tunnels occupied by K^+ ions are larger for the KMWP than KTP and therefore the average potassium-oxygen bond length is much larger in KMWP [3.356 Å at 773 K (Ref. 12)] than in KTP [2.925 Å at 300 K (Ref. 32)]. Our recent Brillouin studies also revealed that the KMWP is a significantly softer material than KTP.[13,14]

Although the lowest wave number mode near 57 cm^{-1} exhibits a clear softening upon approaching the critical pressure P_c, it does not soften to zero and exhibits a sudden shift at P_c. Very similar behavior was also observed previously for KTP.[7] However, the observed softening of the lowest wave number mode of KMWP is much weaker than that observed in KTP, i.e., the pressure derivative for this mode is only −116.3 cm^{-2} GPa^{-1} for KMWP whereas it is −294.0 cm^{-2} GPa^{-1} for KTP.[7] The observed sudden shift of the lowest wave number mode at P_c indicates first-order character of the pressure-induced phase transition. It is worthwhile to note, however, that this shift (about 5.4 cm^{-1}) is much weaker than that observed in KTP (10.9 cm^{-1}),[7] thus indicating a less pronounced first-order character of the pressure-induced phase transition in KMWP. Since the square of this mode wave number is found to be a linear function of pressure, a mean-field-like description seems to be appropriate and the phase transition at 2.0 GPa appears to be driven by the soft mode. A question that arises is what are the symmetry changes at the phase transition. First of all it is worthwhile to note that the Raman spectra of the high-pressure phase are strongly depolarized and the number of the observed modes does not decrease above 2.0 GPa. This result suggests that symmetry changes are weak and the crystal does not transform to the tetragonal or orthorhombic phases observed at ambient pressure and high temperatures. The observation of the soft mode could suggest a group-subgroup relationship between the low- and high-pressure phases. In such case the transition from the ambient pressure P1 symmetry could lead to C_i, C_s, C_2, or C_{2h} structures. Since the soft mode is observed in both low- and high-pressure phases, the pressure-induced phase transition is a Γ-point transition. Transition into a C_i structure can be excluded since in this case the symmetry-breaking order parameter would have A_u symmetry in the high-pressure phase and the soft mode would not be Raman active. The soft mode would be Raman active if symmetry of the high-pressure phase is C_s, C_2, or C_{2h}. This soft mode should be observed in the high-pressure phase in crossed polarization and in the ambient-pressure phase in all polarizations. Therefore in our unpolarized experiment, this mode should exhibit intensity decrease above P_c. Figure 4 shows that this behavior is indeed observed.

Let us now shortly discuss the possibility that the pressure-induced phase transition in KMWP is isosymmetric. Isosymmetric transitions can be induced by instability of an identity-representation mode and they are necessarily first-

order in nature.[33–35] It has been shown, however, that in some cases an isosymmetric transition may be close to second-order.[34] The unstable mode may exhibit softening and change of slope at the phase transition. For instance, a complete softening of the c_{11} elastic constant (and the corresponding longitudinal-acoustic mode) is predicted at the isosymmetric phase transition in sillimanite.[35] As discussed above, the softening of the lowest wave number mode near the pressure-induced isosymmetric phase transition was also observed in KTP.[7] Since KMWP has similar framework as the structure of KTP, and the pressure dependence of Raman modes of KTP and KMWP shows many similarities, it is likely that the pressure-induced transition in KMWP is also isosymmetric. We conclude, therefore, that although the pressure dependence of the Raman modes may be explained assuming a group-subgroup relation between the low- and high-pressure phases, we cannot entirely exclude possibility that the pressure-induced phase transition in KMWP is isosymmetric.

IV. CONCLUSIONS

The ambient-pressure polarized Raman and IR studies as well as LD calculations allowed to propose assignment of the observed bands to respective motions of ions. They showed that the lowest wave number mode can be attributed to translational motions of the K^+ ions along the tunnels. This mode softens as the pressure increases and it plays a major role at the pressure-induced phase transition, which takes place at about 2.0 GPa. This phase transition has a first-order and presumably displacive character. The structural changes at the phase transition are relatively weak. Our results indicate that either symmetry of the high-pressure phase remains the same as symmetry of the ambient-pressure phase, i.e., triclinic P1, or it increases to monoclinic. Discrimination between these two possibilities requires further experimental and theoretical studies. On the basis of the obtained results we were also able to show that this transition is associated with tilts of the PO_4^{3-}, WO_6, and MgO_6 groups.

The pressure-induced phase transitions in KTP and KMWP seem to have a similar character, i.e., they are related to tilting of the polyhedra and are driven by instabilities of the lowest wave number modes which involve translational motions of the K^+ ions. However, KMWP experiences the structural transformation at significantly lower pressure, the pressure dependence of the soft mode is much weaker than that observed for KTP and the first-order character of the phase transition is less pronounced.

ACKNOWLEDGMENTS

M. Maczka acknowledges Departamento de Fisica for supporting the visit to UFC. The Brazilian authors acknowledge financial support from CNPq, CAPES, FUNCAP, and FINEP agencies. W. Paraguassu acknowledges CENAPAD—Campinas for allowing the use of its computational facilities

[1] G. D. Stucky, M. L. F. Phillips, and T. E. Gier, Chem. Mater. **1**, 492 (1989).
[2] J. Hellstrom, V. Pasiskevicius, F. Laurell, and H. Karlsson, Opt. Lett. **24**, 1233 (1999).
[3] Q. Jiang, P. A. Thomas, K. B. Hutton, and R. C. C. Ward, Appl. Phys. Lett. **92**, 2717 (2002).
[4] V. K. Yanovskii and V. I. Voronkova, Phys. Status Solidi A **93**, 99 (1980).
[5] R. V. Pisarev, R. Farhi, P. Moch, and V. I. Voronkova, J. Phys.: Condens. Matter **2**, 7555 (1990).
[6] M. Serhane, C. Dugautier, R. Farhi, P. Moch, and R. V. Pisarev, Ferroelectrics **124**, 373 (1991).
[7] G. A. Kourouklis, A. Jayaraman, and A. A. Ballman, Solid State Commun. **62**, 379 (1987).
[8] D. R. Allan and R. J. Nelmes, J. Phys.: Condens. Matter **8**, 2337 (1996).
[9] E. L. Belokoneva, K. S. Knight, W. I. F. David, and B. V. Mill, J. Phys.: Condens. Matter **9**, 3833 (1997).
[10] U. Peuchert, Ph.D. thesis, University of Cologne, 1995.
[11] U. Peuchert, L. Bohaty, and J. Schreuer, Acta Crystallogr., Sect. C: Cryst. Struct. Commun. **53**, 11 (1997).
[12] U. Peuchert, L. Bohaty, and J. Schreuer, J. Appl. Crystallogr. **31**, 10 (1998).
[13] M. Maczka, J. Hanuza, A. Majchrowski, and S. Kojima, Appl. Phys. Lett. **90**, 122903 (2007).
[14] M. Maczka, J. Hanuza, A. Majchrowski, and S. Kojima, Phys. Rev. B **75**, 214105 (2007).
[15] F. Gervais and P. Echegut, in *Incommensurate Phases in Dielectrics*, edited by R. Blinc and A. P. Levanyuk (North-Holland, Amsterdam, 1986), p. 337.
[16] J. D. Gale, Philos. Mag. Lett. **73**, 3 (1996).
[17] J. D. Gale, J. Chem. Soc., Faraday Trans. **93**, 629 (1997).
[18] E. Dowty, Phys. Chem. Miner. **14**, 67 (1987).
[19] G. E. Kugel, F. Brehat, B. Wyncke, M. D. Fontana, G. Marnier, C. Carabatos-Nedelec, and J. Mangin, J. Phys. C **21**, 5565 (1988).
[20] C.-S. Tu, A. R. Guo, R. Tao, and R. S. Katiyar, J. Appl. Phys. **79**, 3235 (1996).
[21] K. Vivekanandan, S. Selvasekarapandian, P. Kolandaivel, M. T. Sebastian, and S. Suma, Mater. Chem. Phys. **49**, 204 (1997).
[22] M. J. Bushiri, R. S. Jayasree, M. Fakhfakh, and V. U. Nayar, Mater. Chem. Phys. **73**, 179 (2002).
[23] M. J. Bushiri and V. U. Nayar, J. Nonlinear Opt. Phys. Mater. **10**, 345 (2001).
[24] M. Barj, G. Lucazeau, and C. Delmas, J. Solid State Chem. **100**, 141 (1992).
[25] K. Nakamoto, *Infrared and Raman Spectra of Inorganic and Coordination Compounds* (Wiley, New York, 1986).
[26] L. Benarafa, L. Rghioui, R. Nejjar, M. Saidi Idrissi, M. Knidiri, A. Loriaux, and F. Wallart, Spectrochim. Acta, Part A **61**, 419 (2005).
[27] M. J. Bushiri, V. P. Mahadevan Pillai, R. Ratheesh, and V. U. Nayar, J. Phys. Chem. Solids **60**, 1983 (1999).
[28] E. Husson, F. Genet, A. Lachgar, and Y. Piffard, J. Solid State

Chem. **75**, 305 (1988).
[29] M. Liegeois-Duyckaerts and P. Tarte, Spectrochim. Acta, Part A **30**, 1771 (1974).
[30] M. Maczka, J. Solid State Chem. **129**, 287 (1997).
[31] M. Maczka, J. Hanuza, A. F. Fuentes, and Y. Morioka, J. Phys.: Condens. Matter **16**, 2297 (2004).
[32] P. Delarue, C. Lecomte, M. Jannin, G. Marnier, and B. Menaert, J. Phys.: Condens. Matter **11**, 4123 (1999).
[33] A. G. Christy, Acta Crystallogr., Sect. B: Struct. Sci. **51**, 753 (1995).
[34] I. P. Swainson, R. P. Hammond, J. K. Cockcroft, and R. D. Weir, Phys. Rev. B **66**, 174109 (2002).
[35] A. R. Oganov, G. D. Price, and J. P. Brodholt, Acta Crystallogr., Sect. A: Found. Crystallogr. **57**, 548 (2001).